Iterative Modifications to Snell's Law

Joseph Babcanec*, Benjamin Campbell**

University of South Carolina

***Robert Morris University*

Abstract

At its core, the study of Risley Prism laser beam steering systems relies on concentrated light being refracted through a series of different mediums with varying refractive indices. This paper aims to look at iterated refraction at the elementary particle level, and then propose a robust generalized model for laser beams through rotating objects about a principle axis with arbitrary surfaces on $\mathbb{R}^3$, and even $\mathbb{R}^n$. Generalizations can be reduced by application of wedges, optical focuses, and the like.

Keywords: Refraction, Iteration, Steering Systems

1. Introduction and Background

Optical wedges, also commonly called prisms, are often seen as plates of transparent material with one or both sides having a normal vector that is not orthogonal to the optical axis of the system. When a beam of light encounters an interface that is non-orthogonal, it is refracted, which in simplest terms can be calculated by Snells Law. The amount of refraction is easily calculated for a single stationary wedge, but there are many applications which require understanding of a multi-wedge system in which each wedge can be independently rotating. Using ray tracing it is possible to construct a simplistic but effective model of the beam path traced out when a laser is directed through a series of spinning wedges.

Shortly after their invention 50 years ago lasers were quickly realized to be an ideal tool for manufacturing, replacing some traditional methods of cutting and drilling, and creating opportunities for new types of materials processing. One area where lasers have been very successful is in hole drilling. A laser can produce holes smaller than a conventional drill bit, and can create hole geometries that are otherwise difficult to achieve. In addition, unlike a drill bit, a laser will never become dull. Because of the advantages of laser processing, there is interest in new methods of beam control to produce unique features such as straight and tapered holes.

Optical systems incorporating spinning wedges are now emerging on the market as tools for laser machining, with a two wedge system available from Laser Mech Inc. and a spinning dove prism system from ExOne Co. Work has been done by a Fraunhofer Institute in Germany that has led to the development of a prototype wedge device., A diagram of the four-wedge system available at the Electro-Optics Center is shown in Fig. 1. The origins of the prism pair for beam steering can be traced back to optometry in the late 1800s. A pair of optical wedges is known as a Risley Prism Pair after the Philadelphia Optometrist, Samuel Doty Risley, put two optical wedges in mounts that could be rotated separately. He named his invention Risleys Rotary Prism. The prisms could be easily rotated to measure the how much optical muscles were out of balance which could cause the image formed by each eye to have a vertical or horizontal displacement. Risleys invention sped up the diagnosis of this malady and replaced a large set of prisms that were previously used.

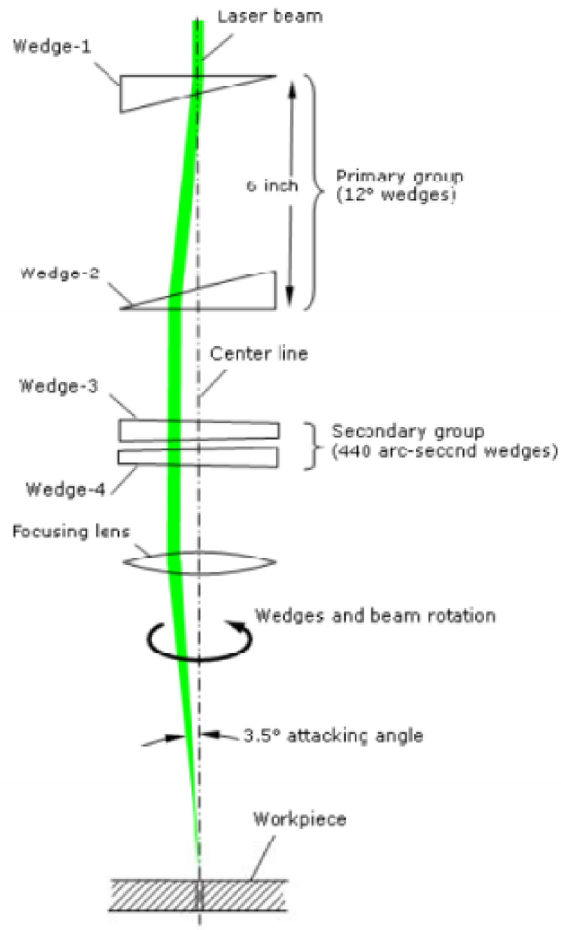

Figure 1: Four-wedge system at Electro-Optics Center

Many types of Risley prism pairs have been adapted for uses outside ophthalmology, most notably for steering a laser beam. The most ubiquitous application with lasers is the bar code scanners found in most retail stores. The Risley prisms have been used in laser and light based detection and ranging (LADAR/LIDAR). They have also been applied to Laser Doppler Vibrometry to measure the velocity of targets at a distance. Various physical models exist to describe the effects of the prisms on rays of light that pass through.

With a simple two prism system, there are two solutions for every desired beam location, but by adding a third wedge, the potential configurations for a desired endpoint become infinite. Adding the third wedge also removes a singularity that occurs when the beam must move through the center of the wedge system, and certain paths require an instantaneous 90 degree turn of one wedge. Detailed third-order beam propagation through a Risley Prism Pair has been conducted recently to show the deviation from the first order approximation. For far field laser scanning applications with Risley prisms, (such as beam correctors for high power laser systems or stabilizers for astronomical spectrometers) the distance to the target is considered to be much greater than the distance between wedges. When deriving the beam path, the disparity in distances often makes the wedge spacing inconsequential. But for applications where the target is within an order of magnitude of the wedge spacing distance, this value becomes significant. With situations that involve more than two wedges in the system, the wedge spacing becomes critical for accurately determining the beam path.

Research efforts have been made to take a desired beam trace and back calculate the parameters needed to produce this shape for a two wedge system. This is a complex problem that requires the use of numerical iteration methods. It has been demonstrated that solutions can be found for rotational angles that take an incident beam and produce a desired set of output conditions. Because of the additional complexity and number of free parameters as additional wedges are added, the range of capabilities is not fully known and merits additional study. While literature describing two wedge systems exists, it has yet to be seen if a 4 wedge model exists that accounts for the distance between wedges and near field targets. The companies that offer the spinning wedge systems them have very little literature available on their capabilities and the tools have not been commercially available long enough to have any significant studies conducted on their performance.

For preliminary design of an optical scanning system, wedges can be approximated as thin prisms as long as the index of refection and the refracting angles are small. But error would grow with each additional prism added to the system. An existing model by G.F. Marshall is a basic tool for demonstrating the ability of wedge pairs to deflect a laser beam. The model very simple and is not well suited for practical studies. First it uses a small angle approximation which introduces errors when using large angle wedges and compounds with each additional element added. Second, it inaccurately represents hole taper because the model does not incorporate distance between the wedges and target, tracing a generalized path with no way to predict size or change of beam path size with distance. Third, there is no allowance for a misaligned beam, it assumes perfect alignment, which is difficult to achieve. Lastly, Marshalls work only uses two wedges but does predict that a four wedge system would be a more elegant solution to make sharper corners on polygons. However, the four wedge system has not been modeled or experimentally verified.

2. Generalized Refraction for Flat Interfaces in $\mathbb{R}^n$

2.1. Directionality and Angles Analysis

In two dimensional Euclidean space, we may naively use basic trigonometry for specific cases to obtain angular information. We begin by employing Snell's Law to provide an output angle to the horizontal x-axis. We will first start with the basic formula for input angle θ_1 and initial refractive index n_1 to an output angle θ_2 with final refractive index n_2:

$$n_1 \sin(\theta_1) = n_2 \sin(\theta_2)$$

While the simplified model works for output angles, this does not speak much to the directionality of the ray generated by a source. We can begin to work with an example interface in

$\mathbb{R}^3$ given by an elementary figure with planar face given by the equation $\Pi := \sum_{j=1}^{3} c_j x_j = 0$ (for coefficients c):

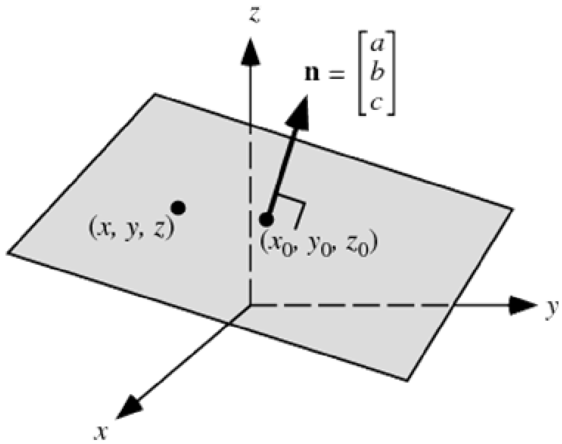

More generally, we have for the planar equation $\Pi := \sum_{j=1}^{n} c_j x_j = 0$ Because we are assuming flat interfaces, we may begin to assign angles for instant moment of rotation with respect to a rotation around a principle axis, say x_* and denoted with rotational matrix R_*. We call these initial angles ϕ_x, ϕ_y in $\mathbb{R}^3$. And for any generalization in n-dimensional Euclidean space, $\phi_1, ..., \phi_{n-1} \in \mathbf{\Phi}$. The rotational angle given by a time dependence for a given rotational speed ω:

$$\gamma = 2\pi\omega t$$

We can begin using vectors to describe directionality now. We will deal with normal vectors to the surface and for unit vectors for each axis (except the principle axis) in $\mathbb{R}^n$ respectively $\hat{\boldsymbol{n}}_\Pi, \hat{\boldsymbol{n}}_1, ..., \hat{\boldsymbol{n}}_{n-1} \in L^2(\mathbb{R}^n)$, for an inner product subspace $L^2(\mathbb{R}^n)$ equipped with the map $\langle \cdot, \cdot \rangle : \boldsymbol{V} \times \boldsymbol{V} \to \mathbb{R}$ and 2-norm $\| \cdot \|_2$. Therefore we may calculate the new changed angles from a rotation around principle axis given by

$$R_*(\gamma) = \begin{bmatrix} \cos(\gamma) & -\sin(\gamma) & \cdots & 0 \\ \sin(\gamma) & \cos(\gamma) & \cdots & 0 \\ \vdots & \vdots & \ddots & \vdots \\ 0 & 0 & \cdots & 1 \end{bmatrix}_{n \times n}$$

Therefore we have for our changed angle vectors for our interface

$$\overline{\mathbf{\Phi}} = \begin{bmatrix} \overline{\phi}_1 \\ \overline{\phi}_2 \\ \vdots \\ \overline{\phi}_{n-2} \\ \overline{\phi}_{n-1} \end{bmatrix} = \begin{bmatrix} \arccos\left(\frac{\langle R_*(\gamma)\hat{\boldsymbol{n}}_\Pi, \hat{\boldsymbol{n}}_1 \rangle}{\|R_*(\gamma)\hat{\boldsymbol{n}}_\Pi\|_2 \|\hat{\boldsymbol{n}}_1\|_2}\right) \\ \arccos\left(\frac{\langle R_*(\gamma)\hat{\boldsymbol{n}}_\Pi, \hat{\boldsymbol{n}}_2 \rangle}{\|R_*(\gamma)\hat{\boldsymbol{n}}_\Pi\|_2 \|\hat{\boldsymbol{n}}_2\|_2}\right) \\ \vdots \\ \arccos\left(\frac{\langle R_*(\gamma)\hat{\boldsymbol{n}}_\Pi, \hat{\boldsymbol{n}}_{n-2} \rangle}{\|R_*(\gamma)\hat{\boldsymbol{n}}_\Pi\|_2 \|\hat{\boldsymbol{n}}_{n-2}\|_2}\right) \\ \arccos\left(\frac{\langle R_*(\gamma)\hat{\boldsymbol{n}}_\Pi, \hat{\boldsymbol{n}}_{n-1} \rangle}{\|R_*(\gamma)\hat{\boldsymbol{n}}_\Pi\|_2 \|\hat{\boldsymbol{n}}_{n-1}\|_2}\right) \end{bmatrix}$$

Note that given the plane equation (or as we will see any surface), Π, we may obtain $\hat{\boldsymbol{n}}_\Pi$ by

$$\nabla\Pi = \begin{bmatrix} c_1 \\ \vdots \\ c_n \end{bmatrix}$$

As an initial condition, we have for $\frac{n}{2}$ many wedges or n many interfaces, the planar angle matrix $\boldsymbol{\Xi}_{n-1\times n+1}$ that for any point in time t_j in a time-series (which will later be formally defined), our transformed matrix at a certain time step is denoted by $\overline{\boldsymbol{\Xi}}_{t_j}$

2.2. Transmission

Now that directionality has been established for the pertinent angles of a workpiece given angle vector $\boldsymbol{\Phi}$, we may now modify Snell's Law to obtain the output angles in any dimension we wish. To motivate this, we begin with new vectors $\boldsymbol{T}, \boldsymbol{I} \in L^2(\mathbb{R}^n)$ to represent the interface and transmission vectors. Let $\boldsymbol{N} \in L^2(\mathbb{R}^n)$ represent a general normal vector to a surface. We will temporarily restrict our vision to the production of a new angle through trasmission just once. We can denote these interior angles as $\theta_i \in \boldsymbol{\Theta}$ and output angle $\overline{\theta_i}$. As an example we can consult the diagram below:

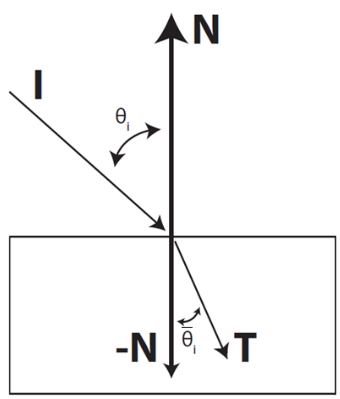

Since the act of transmission that produces the changed variables is dependent physically on refractive indices, we will introduce these indices as n_1, n_2, later to be $n_1, n_2, ..., n_j$ given $n-1$ many iterations. As we derive this new output angle $\overline{\theta}_i$, we will assume that $\boldsymbol{I} := \frac{\boldsymbol{I}}{\|\boldsymbol{I}\|_2}$, $\boldsymbol{T} := \frac{\boldsymbol{T}}{\|\boldsymbol{T}\|_2}$, and $\boldsymbol{N} := \frac{\boldsymbol{N}}{\|\boldsymbol{N}\|_2}$. The negativity of $\boldsymbol{N}$ referring to the directionality as is standard in a vector subspace.

Theorem 1. *Let r be the ratio of two adjacent refractive indices. The refractive transmission vector $\boldsymbol{T}$ off plane Π in $L^2(\mathbb{R}^n)$ subspace is given by*

$$\boldsymbol{T} = r\boldsymbol{I} - \left[r\langle\boldsymbol{N},\boldsymbol{I}\rangle + \sqrt{1 + r^2\left(\langle\boldsymbol{N},\boldsymbol{I}\rangle^2 - 1\right)}\right]\boldsymbol{N}$$

Proof. We may assume the transmission $\boldsymbol{T}$ is a linear combination of the incoming and outgoing rays, that is for two constants $a, b \in \mathbb{R}$, $\boldsymbol{T} = a\boldsymbol{I} + b\boldsymbol{N}$. Begin with Snell's Law and modify to accommodate an arbitrary dimension:

$$r\sin(\theta_i) = \sin(\overline{\theta}_i)$$

$$\Rightarrow r^2\left[1-\langle \boldsymbol{N},\boldsymbol{I}\rangle^2\right]=\left[1-\langle \boldsymbol{N},\boldsymbol{I}\rangle^2\right]$$
$$\Rightarrow r^2\left[1-\langle \boldsymbol{N},\boldsymbol{I}\rangle^2\right]=\left[1-\left(a\langle \boldsymbol{N},\boldsymbol{I}\rangle+b\right)^2\right]$$
$$\Rightarrow 1-r^2\left[1-\langle \boldsymbol{N},\boldsymbol{I}\rangle^2\right]=\left[a\langle \boldsymbol{N},\boldsymbol{I}\rangle\right]^2+2ab\langle \boldsymbol{N},\boldsymbol{I}\rangle+b^2 \tag{1}$$

Taking advantage of our assumptions with our vectors automatically being 2-norms, we can construct

$$1=\langle \boldsymbol{T},\boldsymbol{T}\rangle=\langle (a\boldsymbol{I}+b\boldsymbol{N}),(a\boldsymbol{I}+b\boldsymbol{N})\rangle$$
$$\Rightarrow 1=a^2+2ab\langle \boldsymbol{N},\boldsymbol{I}\rangle+b^2$$
$$\Rightarrow 2ab\langle \boldsymbol{N},\boldsymbol{I}\rangle+b^2=1-a^2 \tag{2}$$

We then have (1) $\rightarrow$ (2) to yield

$$1-r^2\left[1-\langle \boldsymbol{N},\boldsymbol{I}\rangle^2\right]=\left[a\langle \boldsymbol{N},\boldsymbol{I}\rangle\right]^2+\left(1-a^2\right)$$
$$\Rightarrow -r^2\left[1-\langle \boldsymbol{N},\boldsymbol{I}\rangle^2\right]=a^2\left[1-\langle \boldsymbol{N},\boldsymbol{I}\rangle^2\right]$$

By physical nature, $n_1, n_2 > 0$. Therefore we have our first coefficient $a = r$. Consider (2) with the substitution for our first coefficient.

$$2rb\langle \boldsymbol{N},\boldsymbol{I}\rangle+b^2+r^2=1$$

We can see this is quadratic with respect to b. Hence we arrive our the relation

$$b=-r\langle \boldsymbol{N},\boldsymbol{I}\rangle\pm\sqrt{1+r^2\left(\langle \boldsymbol{N},\boldsymbol{I}\rangle^2-1\right)}$$

Because we have that our coefficient b is attached to the normal of the interface, we want to ensure that we have negativity on $\boldsymbol{N}$, therefore to ensure this, we take the negative value for the second term to ensure $b < 0$ regardless of the definition of our vectors. Hence, in this form, we arrive at the desired

$$\boldsymbol{T}=r\boldsymbol{I}-\left[r\langle \boldsymbol{N},\boldsymbol{I}\rangle+\sqrt{1+r^2\left(\langle \boldsymbol{N},\boldsymbol{I}\rangle^2-1\right)}\right]\boldsymbol{N}$$

$\square$

With the directionality and rotational dependent angles well understood, we may now find precise output beams which are fit for iteration. Note that, while we only deal with an arbitrary θ_i, we take this process for each $1 \leq i \leq n$ also as an iteration.

2.3. Single and Multiple Iteration Refractive Process

Let us once again momentarily restrict our vision to $\mathbb{R}^3$ in the below diagram. for $\mathbb{R}^n$, we will now call all unit directions by $x_1, x_2, ..., x_n$, where the principle direction is replaced by the notation x_*. For an incoming ray given by the scheme in $\mathbb{R}^3$, fix the value x_*, Hence $\tan(\theta_i) = \frac{x_i}{x_*}$:

Therefore we may construct $\boldsymbol{I}$, $\boldsymbol{N}$ based off these assumptions. We however apply the same technique for $\boldsymbol{N}$ to be in respect to the $\overline{\phi}_i$ value (since the beam will hit at a certain rotation point). For the purpose of iteration of our process to complete on refractory period

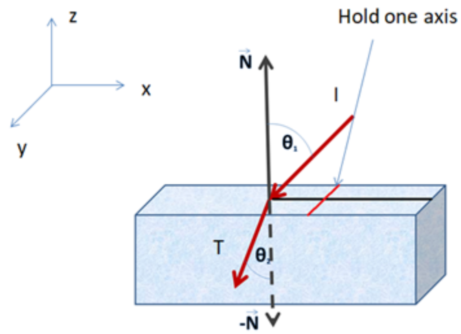

in $\mathbb{R}^n$, let the outer subscript to denote the row in which the entry appears for $1 \leq i \leq n-1$, and let the subscript on the vector reference the angles dimension.

$$\boldsymbol{I}_i = \begin{bmatrix} 0 \\ \vdots \\ x_* \tan(\theta_i)_i \\ 0 \\ \vdots \\ x_* \end{bmatrix}_{n\times 1} \propto \begin{bmatrix} 0 \\ \vdots \\ \tan(\theta_i)_i \\ 0 \\ \vdots \\ 1 \end{bmatrix}, \quad \boldsymbol{N}_i = \begin{bmatrix} 0 \\ \vdots \\ x_* \tan(\overline{\phi}_i)_i \\ 0 \\ \vdots \\ -x_* \end{bmatrix}_{n\times 1} \propto \begin{bmatrix} 0 \\ \vdots \\ \tan(\overline{\phi}_i)_i \\ 0 \\ \vdots \\ -1 \end{bmatrix}$$

We however know that given the 2-norm condition, we may drop the x_* coefficient. For all $\overline{\phi}_i \in \overline{\boldsymbol{\Phi}}$, we may find the angle between the transmission and the normal vector with respect to the principle axis. The only contingency now is that we must extract the sign from the output transmission to find the exact scalar value of $\overline{\theta_i}$. We only need the sign from the coordinate of our principle axis. Define the function $\operatorname{sgn}_*(\cdot) : \boldsymbol{V} \to (\mathbb{Z} \cap [-1, 1])$ to be the standard signum function for that coordinate.

Therefore we can construct a vector, we will say for all $\overline{\theta_i} \in \overline{\boldsymbol{\Theta}}$. This is given by our transmission equation in the following vector. It should be noted that we will address $\boldsymbol{T}_i$ to denote the corresponding index to the incoming θ_i.

$$\overline{\boldsymbol{\Theta}} = \begin{bmatrix} \overline{\theta}_1 \\ \overline{\theta}_2 \\ \vdots \\ \overline{\theta}_{n-2} \\ \overline{\theta}_{n-1} \end{bmatrix} = \begin{bmatrix} \operatorname{sgn}_*(\boldsymbol{T}_1) \arccos\left(\frac{\langle \boldsymbol{T}_1, \hat{\boldsymbol{n}}_* \rangle}{\|\boldsymbol{T}_1\|_2}\right) \\ \operatorname{sgn}_*(\boldsymbol{T}_2) \arccos\left(\frac{\langle \boldsymbol{T}_2, \hat{\boldsymbol{n}}_* \rangle}{\|\boldsymbol{T}_2\|_2}\right) \\ \vdots \\ \operatorname{sgn}_*(\boldsymbol{T}_{n-2}) \arccos\left(\frac{\langle \boldsymbol{T}_{n-2}, \hat{\boldsymbol{n}}_* \rangle}{\|\boldsymbol{T}_{n-2}\|_2}\right) \\ \operatorname{sgn}_*(\boldsymbol{T}_{n-1}) \arccos\left(\frac{\langle \boldsymbol{T}_{n-1}, \hat{\boldsymbol{n}}_* \rangle}{\|\boldsymbol{T}_{n-1}\|_2}\right) \end{bmatrix}$$

Therefore for each iteration, $\overline{\boldsymbol{\Theta}}$ will be the new $\boldsymbol{\Theta}$.

2.4. Ray Tracing

Since we are dealing with vectors, it is only natural to then conduct the ray tracing for parametric equations of lines. Once again, let $x_1, x_2, ..., x_{n-1}$ define the coordinates for the transmission vector, let $a_1, a_2, ..., a_{n-1}$ to define the coordinates for the normal vector to any plane in $\mathbb{R}^n$, and let $\overline{x}_1, \overline{x}_2, ..., \overline{x}_{n-1}$ to define the intersection point between the transmission vector output and the next interface. We have the general form of a parametric line that we can replace with angles between each of our coordinates and the principle axis. Let $\boldsymbol{T}_{x_i}$ denote the x_i coordinate of the transmission vector.

$$\overline{\boldsymbol{r}} = \begin{bmatrix} \overline{x}_1 \\ \overline{x}_2 \\ \vdots \\ \overline{x}_{n-2} \\ \overline{x}_{n-1} \end{bmatrix} = \begin{bmatrix} x_1 \\ x_2 \\ \vdots \\ x_{n-2} \\ x_{n-1} \end{bmatrix} + t \begin{bmatrix} a_1 \\ a_2 \\ \vdots \\ a_{n-2} \\ a_{n-1} \end{bmatrix} = \begin{bmatrix} \boldsymbol{T}_{x_1} \\ \boldsymbol{T}_{x_2} \\ \vdots \\ \boldsymbol{T}_{x_{n-2}} \\ \boldsymbol{T}_{x_{n-1}} \end{bmatrix} + t \begin{bmatrix} \tan(\overline{\theta}_1) \\ \tan(\overline{\theta}_2) \\ \vdots \\ \tan(\overline{\theta}_{n-2}) \\ \tan(\overline{\theta}_{n-1}) \end{bmatrix}$$

Finally, we have our last necessary equation to come from our plane equation Π. We can then solve for each of our intersection points.

3. Refraction with Non-linear Surfaces

3.1. A Quick Reformulation

We only need to make a few adjustments to extend our idea of refraction to non-linear surfaces. Because we are evaluating our entire system as a photon meeting a contact point on a surface, we can make a few approximations. The only difference will be the fact that we will take a tangent plane for a point on the surface and then calculate the transmission with the generated planar surface just as we have. The difference this time is that we have a few restrictions as to what type of surfaces we may use to approximate.

We first must establish a boundary function B. For this boundary function to work in $\mathbb{R}^n$, we will let it be defined as $B(x_1, ...) \in C[p_*, p^*]^{n-1}$ for some values p_* to be the minimum value of the principal axis and p^* to be the maximum value thereof. B is then rotated around the principal axis. We also must be guaranteed that that for $|B - p_i| \geq \epsilon$ for all points p_i on the principle axis. Therefore we may say that if the constructed ray $\boldsymbol{T}_i = B(R)$ at any point R, the analysis has been defined as indeterminate for the initial conditions for all i.

Now that we have an idea of boundary, we can condition our non-linear surface S.

1. S is differentiable at every all points of contact with the photon for all values γ.
2. S must intersection with B at all points in the rotation of B around the principle axis
3. $S(0, ..., 0, x_*)$ is monotonic.
4. $S \in C[p_*, p^*]$

Therefore we have our linear equation for our intermediary plane that is tangent to the point $Q(x_1^*, x_2^*, ..., x_n^*)$ for which the photon is hitting on the surface:

$$\Pi(Q) := \sum_{j=1}^{n} \frac{\partial S(Q)}{\partial x_i}(x_i - x_i^*) = 0$$

Therefore our iterative refraction has become the identical process as planar surfaces.

4. Beam Projection

4.1. Quantifying Information

Our end goal is to track a photons path up until it hits a certain workpiece. Define another planar function $W(x_1, ..., x_n)$ to be describe this, where every point on this plane is the outer most limit of our subspace. It should be noted that this function is not subject to rotational parameters. We are primarily interested in the set of all n-dimensional points that intersect with W. We can call these intersection points $\rho_j \in \mathbb{R}^n$, and store these in matrix $\mathbf{\Psi}$. Note that each component of ρ_j comes from a single path iterating over the number of interfaces at a specific time step. We can partition our analysis into time steps $t_1 < t_2 < ... < t_k$, for $1 \leq j \leq k$. Therefore when we calculate $\overline{\overline{\mathbf{\Xi}}}_{t_j}$, this corresponds to the points $\rho_i \in \mathbf{\Psi}$. Thus our matrix becomes

$$\mathbf{\Psi} = \begin{bmatrix} \rho_1 & \cdots & \rho_j \end{bmatrix}_{n \times j}$$

4.2. Results in $\mathbb{R}^3$ using MATLAB

5. Conclusion

This paper has provided a very general outlook on how Snell's Law can be modified to fit refraction of rotating wedges in any finite dimension. This therefore can easily be simplified to physical models in $\mathbb{R}^3$ and can therefore be applied to make predictions of beam paths and the projections that arise from the iterated transmission. It should be noted that this paper assumes a number of ideal physical requirements such as infinitesimal and perfectly strong laser profile. This paper also neglects to comment on reflection that occurs naturally from lustrous surfaces, but this calculation becomes very easy given the mathematical foundation that has been set forth.

Future work will now include a robust model for the inverse problem to refraction: finding all prerequisites given the point cloud projected image. As we know the work of [], [], and [] have already explored this avenue, but improvements can be made in the process as the criterion for finding initial conditions is much less robust.

6. Bibliography